

Electronic Supplementary Material

Comparison of extruded cell nanovesicles and exosomes in their molecular cargos and regenerative potentials

Xianyun Wang^{1,2,3,4,5,6}, Shiqi Hu^{5,6}, Dashuai Zhu^{5,6}, Junlang Li^{5,6}, Ke Cheng^{5,6} (✉), and Gang Liu^{1,3,4} (✉)

¹ Department of Cardiology, The First Hospital of Hebei Medical University, Shijiazhuang 050000, China

² Scientific Research Data Center, The First Hospital of Hebei Medical University, Shijiazhuang 050000, China

³ Hebei Key Laboratory of Cardiac Injury Repair Mechanism Study, Shijiazhuang, China

⁴ Hebei International Joint Research Center for Structural Heart Disease, Shijiazhuang 050000, China

⁵ Department of Molecular Biomedical Science, North Carolina State University, Raleigh 27607, North Carolina, USA

⁶ Department of Biomedical Engineering, University of North Carolina, Chapel Hill and North Carolina State University, Raleigh 27607, North Carolina, USA

Supporting information to <https://doi.org/10.1007/s12274-023-5374-3>

(a)

A1, 2	RS(+)	B15, 16	Endothelin-1	D5, 6	IP-10	E13, 14	CXCL4
A7, 8	Amphiregulin	B17, 18	FGF-1	D7, 8	CXCL1	E15, 16	PlGF-2
A9, 10	Angiogenin	B19, 20	FGF-2	D9, 10	Leptin	E17, 18	Prolactin
A11, 12	Ang-1	C3, 4	FGF-7	D11, 12	MCP-1	E19, 20	Proliferin
A13, 14	Ang-3	C5, 6	CX3CL1	D13, 14	CCL3	F1, 2	RS(+)
A15, 16	FIII	C7, 8	GM-CSF	D15, 16	MMP-3	F3, 4	SDF-1
A17, 18	CXCL16	C9, 10	HB-EGF	D17, 18	MMP-8	F5, 6	Serpin E1
A21, 22	RS(+)	C11, 12	HGF	D19, 20	MMP-9	F7, 8	Serpin F1
B3, 4	Cyr61	C13, 14	IGFBP-1	D21, 22	CCN3	F9, 10	TSP2
B5, 6	DLL4	C15, 16	IGFBP-2	E3, 4	Osteopontin	F11, 12	TIMP-1
B7, 8	CD26	C17, 18	IGFBP-3	E5, 6	PD-ECGF	F13, 14	TIMP-4
B9, 10	EGF	C19, 20	IL-1 α	E7, 8	PDGF-AA	F15, 16	VEGF
B11, 12	CD105	C21, 22	IL-1 β	E9, 10	PDGF-AB	F17, 18	VEGF-B
B3,14	Endostatin	D3, 4	IL-10	E11, 12	Pentraxin-3	F19, 20	Cont(-)

(b)

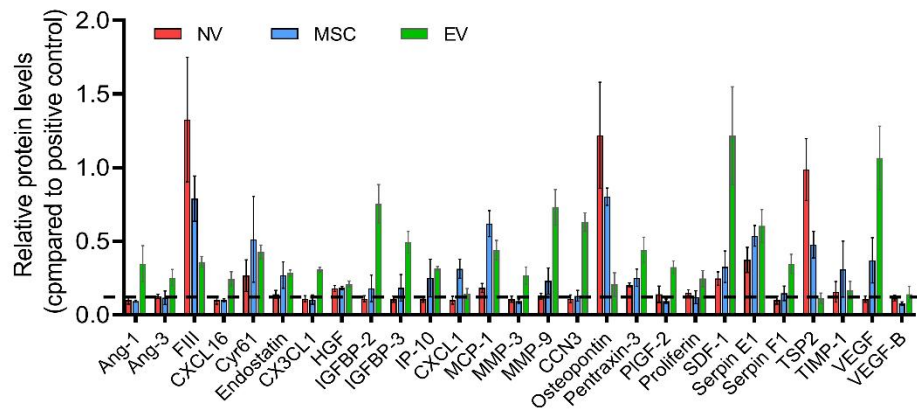


Fig. S1 The position of proteins in a protein array and the analysis of their differential expression levels.

The position of proteins of interest (a) and their expression levels relative to positive control (b). Data are presented as the mean \pm SD of three independent biological samples.

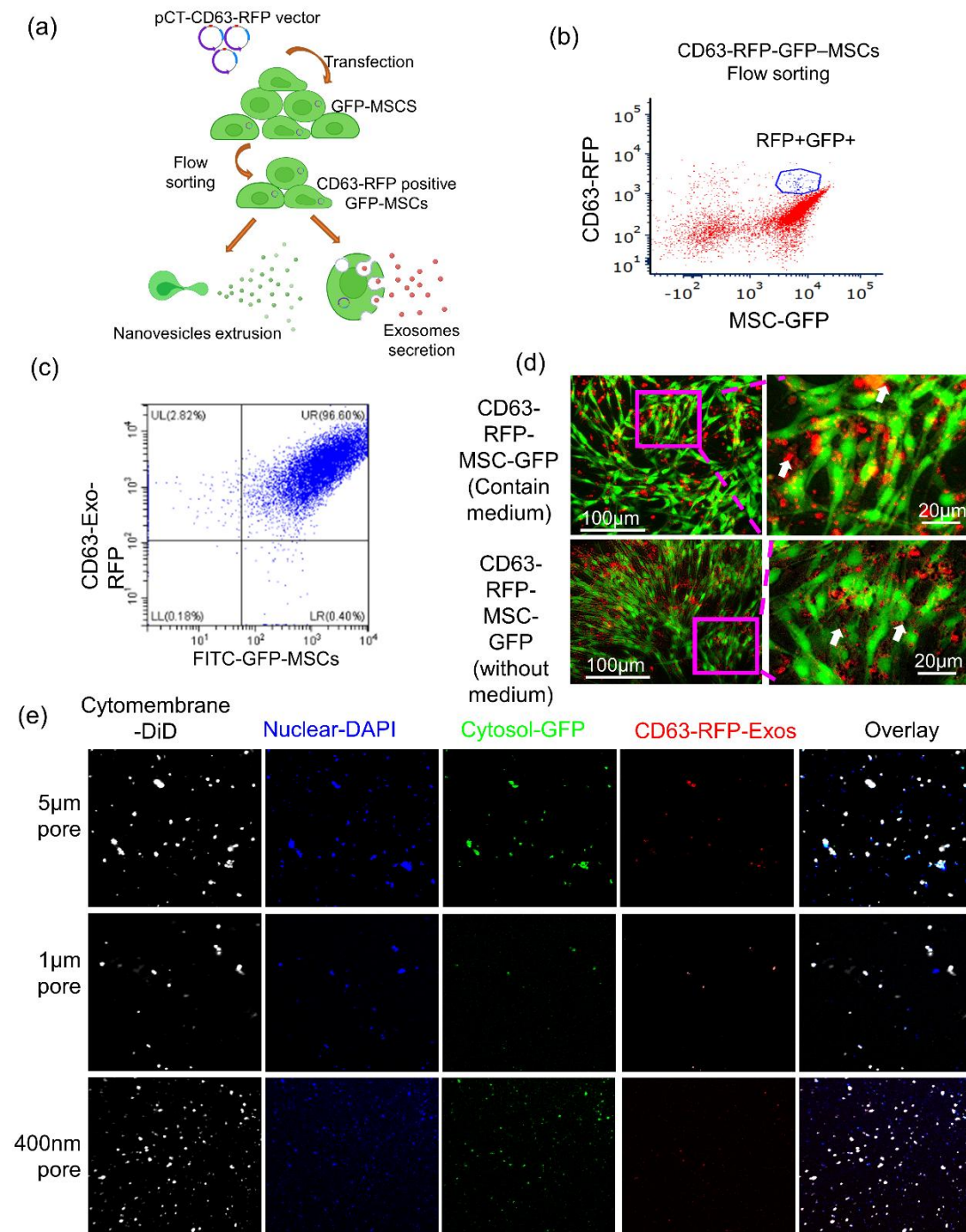


Fig. S2 Construction of the CD63-RFP-expressing exosome GFP-MSC system and the identification of the components of nanovesicles obtained through serial extrusion. (a) A schematic illustration of the construction of the CD63-RFP-exosome GFP-MSC system. (b) Tetraspanin CD63 Cyto-Tracer was transferred into GFP-MSCs and purified by flow sorting. (c) The expression of fluorescent signals in MSCs was measured by flow cytometry. More than 90% of cells were both RFP- and GFP-positive. (d) Tetraspanin CD63-RFP-expressing GFP-MSCs cultured with or without conditioned medium were observed under the immunofluorescence microscope. (e) After the cells were stained with DiD dye, the flow-through following

filtration through each pore size was collected. Cellular nuclei were stained with DAPI. The different fluorescent cell labels such as membrane (DiD), cytoplasm (GFP), exosomes (RFP) and nucleus (DAPI), were observed with a fluorescence confocal microscope. Data are presented as the mean \pm SD of 3-5 independent biological samples.

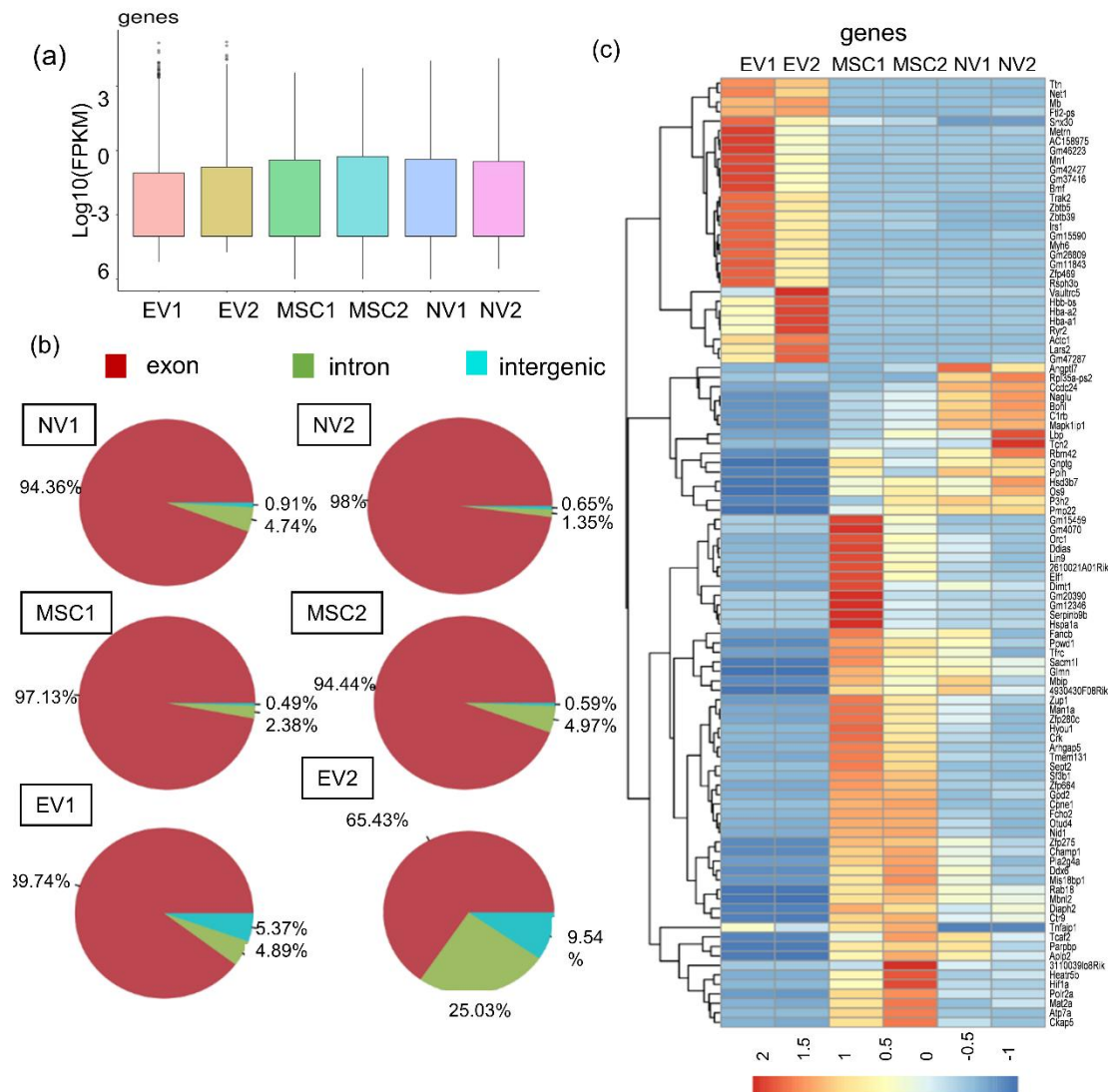


Fig. S3 The differential genomics analysis between the NV, MSC, and EV groups.

(a)–(c) The genetic profile of the NV group was very similar to that of MSC rather than EV, which indicates that NVs inherit the majority of their genetic profile from the components of the MSCs after extrusion. Data are presented as the mean \pm SD of two independent biological samples.

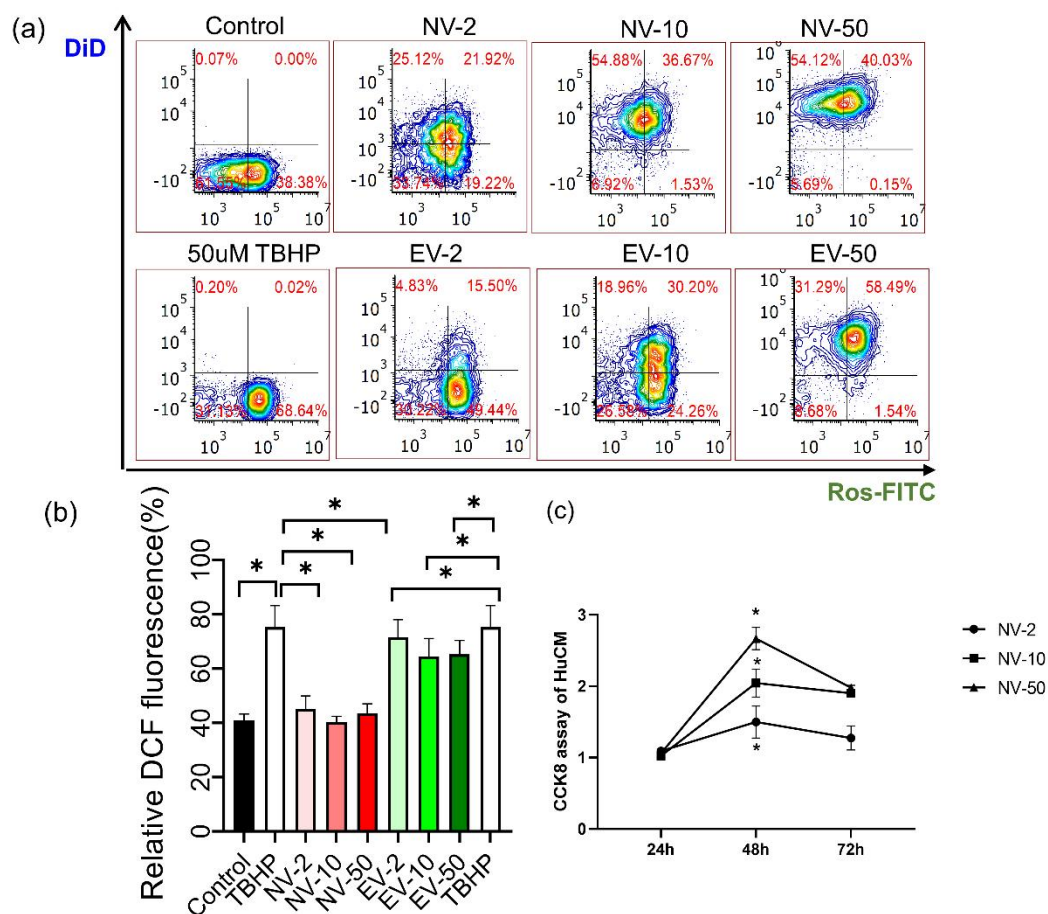


Fig.S4 The protective role of NVs under the stimulation of hydrogen peroxide. ROS level was inhibited in HuCMs after NV pretreatment for 3h ((a) & (b)). The proliferation ability was analyzed by CCK8 assay after 10μg/μl NVs or 2μg/μl EVs stimulation for 24h, 48h, or 72h (c). Data are presented as the mean ± SD of 3 independent biological samples. * $P < 0.05$, # $P < 0.05$.